Electronic Supplementary Material (ESI) for Materials Advances.

Supporting Information

Cationic and Oxygen Defects Modulation for Tailoring Bandgap and Room Temperature Ferromagnetism of CuO via Multiple d-Block Cations

Md Shafayatul Islam[1], Koushik Roy Chowdhury[1], Sheikh Manjura Hoque[2], and Ahmed Sharif1[1]*

[1]Department of Materials and Metallurgical Engineering, Bangladesh University of Engineering and Technology, Dhaka 1000

[2]Materials Science Division, Atomic Energy Centre, Dhaka, Bangladesh

*Email: asharif@mme.buet.ac.bd

Defect Notation

Kröger-Vink notation is used to write simple equations to describe the formation of point defects and their interaction. The necessary explanation of the notation Summary for, S_P^c:

S: Species

P: Position in the crystal

c: Charge relative to the perfect crystal

Charge notation:

- Positive: point ($^{\bullet}$)
- Negative: dash ($'$)
- Neutral: *x*

.

Structural Information

Table S1: Rietveld analysis of pristine CuO, CuO-a, CuO-b and CuO-c samples.

Sample	CuO	CuO-a	CuO-b		CuO-c	
Constituent phases	**CuO**	**CuO**	**CuO**	**Cu**	**CuO**	**Cu**
Space group	C2/c(15)	C2/c(15)	C2/c(15)	Fm-3m(225)	C2/c(15)	Fm-3m(225)
Unit cell parameter	a =4.6853 Å	a = 4.6887 Å	a = 4.6916 Å	a = 3.6062 Å	a =4.6887 Å	a = 3.6195 Å
	b =3.4240 Å	b =3.42 Å	b =3.4211 Å		b = 3.4221 Å	
	c =5.1317 Å	c =5.1295 Å	c =5.1326 Å		c = 5.1292 Å	
	β =99.402°	β = 99.515°	β = 99.471°		β = 99.456°	
	V =81.219 Å^3	V = 81.121 Å^3	V = 81.256 Å^3	V = 46.898 Å^3	V = 81.181 Å^3	V = 47.418 Å^3
Rietveld factors	R_{exp} = 5.845	R_{exp} = 5.360	R_{exp} = 7.011		R_{exp} = 6.464	
	R_p = 6.19956	R_p = 6.25719	R_p = 6.6287		R_p = 6.77898	
	R_{wp} = 8.92747	R_{wp} = 8.34275	R_{wp} = 8.91337		R_{wp} = 9.00301	
	GoF = 2.33	GoF = 2.42	GoF = 1.62		GoF = 1.94	
Cu-O Bond length	1.95943 Å	1.96091 Å	1.96148 Å		1.96018 Å	
Average Cu-O-Cu Bond angle	104.017°	103.946°	103.942°		103.953°	

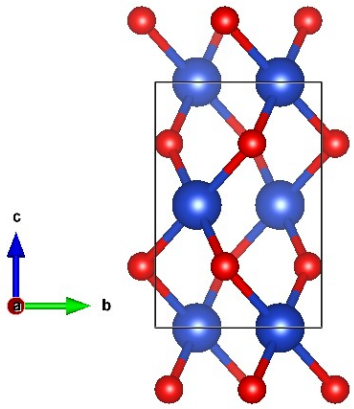

Fig. S1 Monoclinic C2/c structure of CuO NCs.

XPS analysis

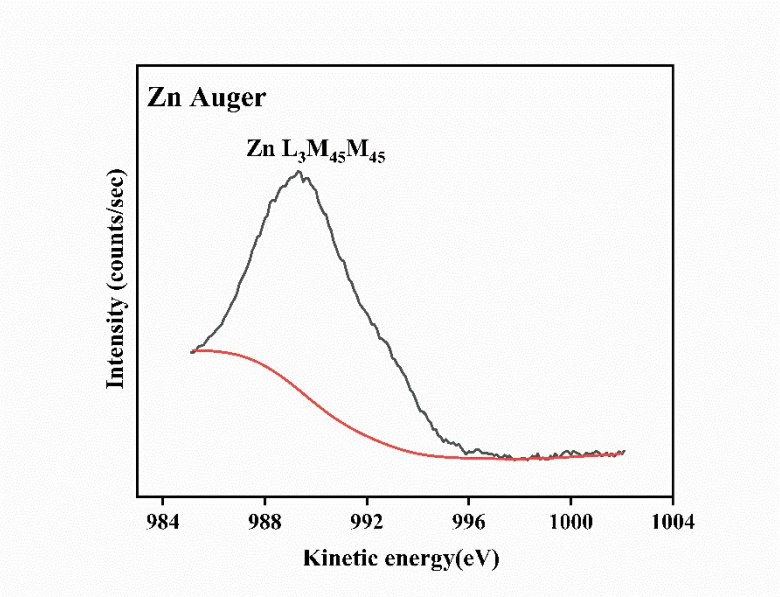

Fig. S2 High-resolution spectrum of the Zn auger peak for CuO-c NCs.

Elemental analysis

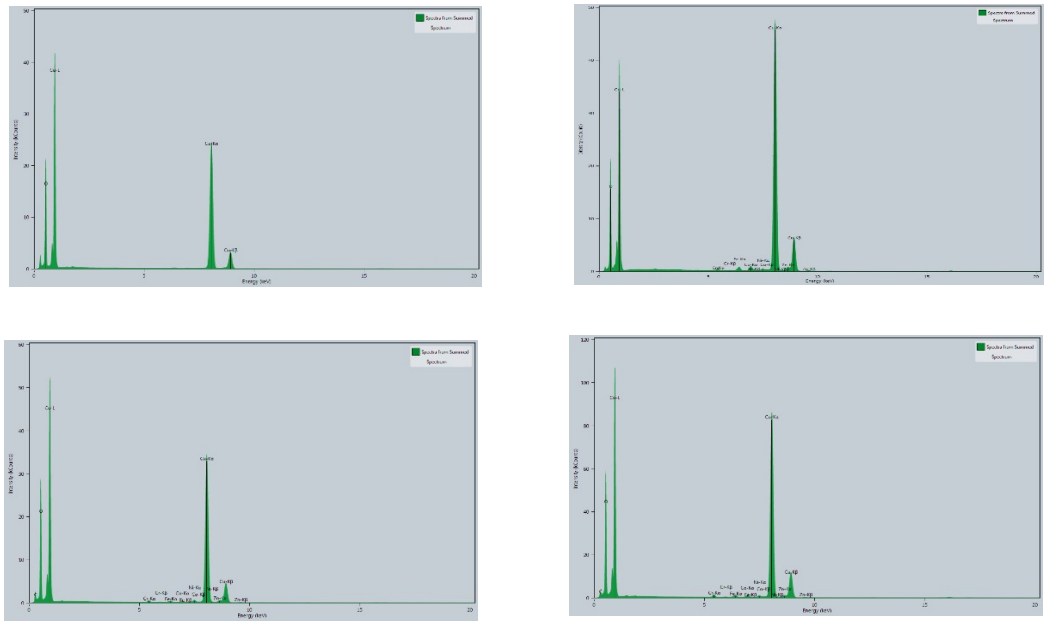

Fig. S3 EDX Spectra of (a) Pristine CuO (b) CuO-a (c) CuO-b, and (d) CuO-c NCs.

Optical properties

Using electronegativity, the geometric mean of the electronegativity of the component atoms, the edges of the conduction and valence bands of semiconductors were determined.

$$\chi = \sqrt[N]{\chi_1^a \chi_2^b \cdots\cdots \chi_{n-1}^u \chi_n^v} \ldots\ldots\ldots\ldots\ldots\ldots S1$$

Where N is the total number of elements in the compound, χ_n is the electronegativity of specific element, and v is the mole fraction[1]. The electronegativity of a specific element is the mean of the ionization potential (IP) and atomic electron affinity (EA)[2]:

$$\chi_n = \frac{IP + EA}{2} \quad \ldots\ldots\ldots\ldots\ldots\ldots S2$$

Table S2: Calculated values of IP, EA, and electronegativity for Cu and O atoms.

Elements	**IP (eV)**	**EA (eV)**	**Electronegativity, χ_n (eV)**
Cu	7.72	1.23	4.48
O	13.62	1.46	7.54

Hence, the electronegativity of CuO NCs using equation S1:

$$\chi_{CuO} = \sqrt[2]{(4.48)_{Cu}^{1}(7.54)_{O}^{1}} = 5.81$$

Magnetic properties

Magnetization (M) – Temperature (T) curves in zero field cooling (ZFC) mode were measured to further investigate the materials' magnetic characteristics at low temperatures (Fig. S4). ZFC magnetization is a metastable condition from a physical perspective, meaning that the relaxation time of the particle moment is often larger than the magnetic measurement time scale[3]. For ZFC mode, the sample was cooled from 400

K to 5 K in the absence of any fields. Magnetization was monitored as temperatures rose from 5 K by applying a small magnetic field of 100 Oe. ZFC curves display a peak-like feature (as shown by the orange arrow in Fig. S4) at around 200, 110.02, 40.1, and 110.02 K for pristine CuO, CuO-a, CuO-b, and CuO-c, respectively, after which the magnetic moments have gained enough thermal energy to flip randomly[4].

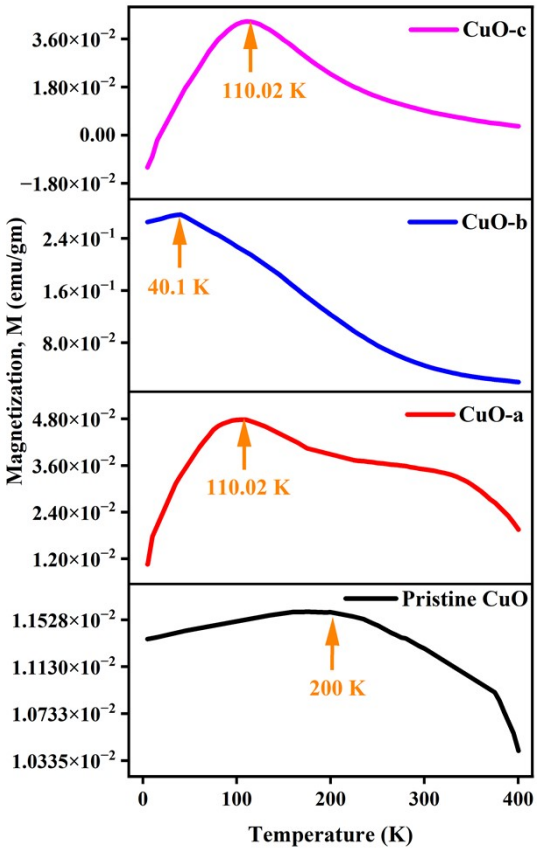

Fig. S4 Thermomagnetization (M–T) curves in ZFC mode

Thus, this peak temperature suggests an initiation of paramagnetism in the inner grains from the antiferromagnetic ordering of the bulk Cu-O-Cu chain[5]. With increasing particle size, the peak in ZFC becomes broader, which explains the broad nature of the pristine CuO peak noticed in ZFC curves[6]. A small amount of negative magnetization is observed at the low-temperature ZFC curve for CuO-c, which can be assigned to remnant magnetization present in the NCs that is not compensated by the 100 Oe field or the trapping of a small negative field in the NCs.

References

(1) Nethercot, A. H. Prediction of Fermi Energies and Photoelectric Thresholds Based on Electronegativity Concepts. *Phys. Rev. Lett.* **1974**, *33* (18), 1088–1091. https://doi.org/10.1103/PhysRevLett.33.1088.

(2) Islam, Md. R.; Zubair, M. A.; Bashar, M. S.; Rashid, A. K. M. B. Bi0.9Ho0.1FeO3/TiO2 Composite Thin Films: Synthesis and Study of Optical, Electrical and Magnetic Properties. *Sci Rep* **2019**, *9* (1), 5205. https://doi.org/10.1038/s41598-019-41570-x.

(3) Paswan, S. K.; Kumari, S.; Kar, M.; Singh, A.; Pathak, H.; Borah, J. P.; Kumar, L. Optimization of Structure-Property Relationships in Nickel Ferrite Nanoparticles Annealed at Different Temperature. *Journal of Physics and Chemistry of Solids* **2021**, *151*, 109928. https://doi.org/10.1016/j.jpcs.2020.109928.

(4) Punnoose, A.; Magnone, H.; Seehra, M. S.; Bonevich, J. Bulk to Nanoscale Magnetism and Exchange Bias in CuO Nanoparticles. *Phys. Rev. B* **2001**, *64* (17), 174420. https://doi.org/10.1103/PhysRevB.64.174420.

(5) Manna, S.; De, S. K. Room Temperature Ferromagnetism in Fe Doped CuO Nanorods. *Journal of Magnetism and Magnetic Materials* **2010**, *322* (18), 2749–2753. https://doi.org/10.1016/j.jmmm.2010.04.020.

(6) Ajroudi, L.; Mliki, N.; Bessais, L.; Madigou, V.; Villain, S.; Leroux, Ch. Magnetic, Electric and Thermal Properties of Cobalt Ferrite Nanoparticles. *Materials Research Bulletin* **2014**, *59*, 49–58. https://doi.org/10.1016/j.materresbull.2014.06.029.